13

Minimum Energy Trajectory Planning for Biped Robots

Yasutaka Fujimoto
Yokohama National University
Japan

1. Introduction

Biped robots have potential ability to elevate mobility of robotic system and they attract general attention in the last decade. Due to their form, it is easy to introduce them into our living space without preparing special infrastructure. There are many theoretical and experimental studies on the biped robots. Recently, several autonomous biped humanoid robots have been developed. In 1996, the first autonomous bipedal humanoid robot with battery power supply was developed by Honda Motor Co., Ltd. (Hirai, et al., 1998). Takanishi and his co-workers at Waseda University built a human-size bipedal humanoid robot and proposed a basic control method of whole body cooperative dynamic biped walking (Yamaguchi et al., 1999). Same group also developed a biped robot having two Stewart platforms as legs (Sugahara, et al., 2003). Kaneko and his colleagues at the National Institute of Advanced Industrial Science and Technology (AIST) also developed a bipedal humanoid robot of 1.54m height and 58kg weight mainly for the purpose of investigating fundamental techniques and applications (Kaneko et al., 2004). Same group also proposed a method of a biped walking pattern generation by using a preview control of the zero-moment point(ZMP) (Kajita, et al., 2003). The ZMP and its extension (FRI; foot-rotation indicator) are basic stability criteria for biped robots (Vukobratovic, et al, 2001, Goswami, 1999). Nishiwaki and his co-researchers at University of Tokyo studied a humanoid walking control system that generates body trajectories to follow a given desired motion online (Nishiwaki, et al. 2003). Loffler and his colleagues at Technical University of Munich also designed a biped robot to achieve a dynamically stable gait pattern (Loffler, et al., 2003).
Generally, careful design is required for development of a bipedal robot. Selection of gears and actuators, taking their rate, power, torque, and weight into account, is especially important. Developments of power conversion technology based on semiconductor switching devices and rare-earth permanent magnet materials Nd-Fe-B in combination with optimal design of the electromagnetic field by the finite element method enable improvement of power/weight ratio of actuators. They contribute to the realization of such autonomous biped robots. However, they are still underpowered to achieve fast walking and running motions as the same that human does. There are several researches on running control of biped model (Raibert, 1986, Hodgins, 1996, Kajita, et al., 2002). The first human-size running robot was developed at AIST (Nagasaki, et al., 2004). In December 2005, Honda Motor Co., Ltd. announced their new bipedal humanoid robot that could run at 6km/h. Kajita, et al. proposed a method to generate a running pattern and reported that it requires

Source: Humanoid Robots, New Developments, Book edited by: Armando Carlos de Pina Filho
ISBN 978-3-902613-02-8, pp.582, I-Tech, Vienna, Austria, June 2007

at least 28 to 56 times more powerful actuators than that of their actual humanoid robot HRP1, and also the consumption power is estimated ten times bigger than the human runner (Kajita, et al., 2002)

In this chapter, a method to generate a trajectory of a running motion with minimum energy consumption is introduced. It is useful to know the lower bound of the consumption energy when we design the biped robot and select actuators. The generation of low-energy trajectories for biped robots remained an open problem. Usually, it is formulated as an optimal control problem. Since symbolic expression of motion equation of robots becomes extremely complicated in the case that the number of links increases, only specific simple type of a structure of robots was investigated and simplified assumptions such as ignoring the effects of centripetal forces were made in the past works (Roussel, et al., 1998). In this chapter, exact and general formulation of optimal control for biped robots based on recursive representation of motion equation is introduced. As an illustrative numerical example, the method is applied to a five link planar biped robot of 1.2m height and 60kg weight. The robot with the generated minimum energy running pattern with 1m/sec speed consumes only 45W on average. It is found that big peak power and torque is required for the knee joints but its consumption power is negative small and the main work is done by the hip joints.

The rest of this chapter is organized as follows. In Section 2, the problem definition is introduced where the formulation of the biped running robot is given. The minimization of consumption energy is explained in the Section 3, and the computational scheme is proposed in the Section 4. The numerical study of a five link planar biped robot is provided in Section 5, and conclusions are outlined in the Section 6.

2. Model of Biped Running Robot

2.1 Basic Model of a Biped Robot

Consider a three dimensional bipedal robot with open-chain mechanism consisting of N joints and N+1 rigid links. Since the robot is not fixed on the ground, it is modelled as a free-fall manipulator which has N+6 motion-degree-of-freedom (Fujimoto & Kawamura, 1995, 1998). The model in general form is given by

$$H\ddot{x} + C\dot{x} + g = u + J^T f_E \tag{1}$$

where $H \in \Re^{(N+6)\times(N+6)}$ is an inertia matrix, $C \in \Re^{(N+6)\times(N+6)}$ specifies centrifugal and Coriolis effects, $g \in \Re^{N+6}$ specifies gravity effects, $x = (\theta, \varphi, p) \in \Re^{N+6}$ specifies displacements of joints, and posture and position of a base link. $u = (n,0,0) \in \Re^{N+6}$ specifies input generalized forces. $f_E \in \Re^6$ is external force and $J \in \Re^{6\times(N+6)}$ is a Jacobian matrix for tip of the support leg. Also $\theta, n \in \Re^N$ specify joint angles and input joint torques, respectively. $\varphi, p \in \Re^{N+3}$ specify posture and position of a base link, respectively. An example of the coordinates for the case of planner biped is shown in Fig. 1.

2.2 Model of Support Phase

The motion of running is decomposed to two phases; single-leg support phase and flight phase.

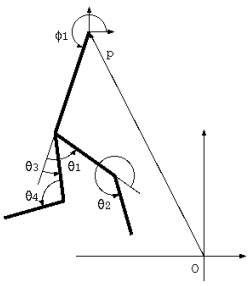

Fig. 1. A five link biped robot.

Let the tip position of the support leg with respect to the origin of the base link system be $h(\theta,\varphi)$. Then its position with respect to the origin of the world coordinate system is represented by

$$y = h(\theta,\varphi) + p \tag{2}$$

Since the foot of the support leg is fixed on the ground during single support phase, it is subject to the following conditions.

$$\dot{y} = J\dot{\theta} + R\dot{\varphi} + \dot{p} = 0 \tag{3}$$

$$\ddot{y} = J\ddot{\theta} + \dot{J}\dot{\theta} + R\ddot{\varphi} + \dot{R}\dot{\varphi} + \ddot{p} = 0 \tag{4}$$

where $J = \partial h / \partial \theta^T$ and $R = \partial h / \partial \varphi^T$ are Jacobian matrices.

Eliminating $\dot{p}$, $\ddot{p}$, and f_E from (1) using (3) and (4), the following dynamics is obtained.

$$H_s\ddot{x}_s + C_s\dot{x}_s + g_s = u_s \tag{5}$$

where $x_s = (\theta_s, \varphi_s)$ and $u_s = (n_s, 0)$. The subscript s represents variables during support phase. The state equation is given by

$$\dot{w}_s = \begin{bmatrix} \dot{x}_s \\ H_s^{-1}(u_s - C_s\dot{x}_s - g_s) \end{bmatrix} \tag{6}$$

where $w_s = (x_s, \dot{x}_s) = (\theta_s, \varphi_s, \dot{\theta}_s, \dot{\varphi}_s) \in \Re^{2N+6}$ is a state vector.

2.3 Model of Flight Phase

During flight phase, the external force f_E in the motion equation (1) is zero. The conservation law of angular momentum is already included equivalently, which corresponds to no existence of external forces. Therefore the dynamics becomes

$$H_f\ddot{x}_f + C_f\dot{x}_f + g_f = u_f \tag{7}$$

where $x_f = (\theta_f, \varphi_f, p_f)$ and $u_f = (n_f, 0, 0)$. The subscript f represents variables during flight phase. The state equation is given by

$$\dot{w}_f = \begin{bmatrix} \dot{x}_f \\ H_f^{-1}(u_f - C_f\dot{x}_f - g_f) \end{bmatrix} \tag{8}$$

where $w_f = (x_f, \dot{x}_f) = (\theta_f, \varphi_f, p, \dot{\theta}_f, \dot{\varphi}_f, \dot{p}) \in \Re^{2(N+6)}$ is a state vector.

3. Generation of Minimum Energy Consumption Gait

It is useful to know the lower bound of the consumption energy when we design the bipedal robot and select actuators. An ideal actuator is assumed in this chapter to investigate the consumption energy, although real actuators with high-ratio gears such as harmonic gears have large frictions and roughly 70% of energy efficiency. The energy regeneration is considered. The problem is to find input joint torques and initial posture that minimize input energy during running motion under the condition that the robot takes completely periodic and symmetric motion, given the step period and the stride. The problem is described as follow.

$$\text{minimize} \quad E = \int_0^T \dot{\theta}^T n dt \tag{9}$$

$$\text{subject to} \begin{cases} \theta(T) = K\theta(0) \\ \varphi(T) = \varphi(0) \\ p(T) = p(0) + S \\ H\ddot{x} + C\dot{x} + g = u + J^T f_E \end{cases} \tag{10}$$

where T is a period for one step. S is the stride. K is a coordinate conversion matrix;

$$K = \begin{bmatrix} I_b & 0 & 0 \\ 0 & 0 & I_\ell \\ 0 & I_\ell & 0 \end{bmatrix} \tag{11}$$

where I_b and I_ℓ are identity matrices whose dimensions are same as number of joints in body and one leg, respectively.

Since the structure of dynamics varies depending on the phase as shown in the previous section, a reflection of time axis is introduced. A new time axis is given by

$$\tau = \begin{cases} \dfrac{t}{\alpha T} & \text{for} \quad 0 \le t \le \alpha T \\ \dfrac{T-t}{(1-\alpha)T} & \text{for} \quad \alpha T \le t \le T \end{cases} \tag{12}$$

The timing chart of events are shown in Fig. 2. All variables in the rest of this section are functions of τ.

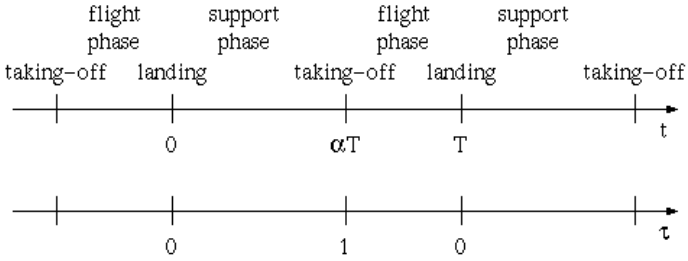

Fig. 2. Timing chart of events.

The objective function (9) is represented by

$$\begin{aligned} E &= \int_0^{\alpha T} \dot{\theta}^T n \, dt + \int_{\alpha T}^{T} \dot{\theta}^T n \, dt \\ &= \int_0^1 \left(\alpha \dot{\theta}_s^T n_s + (1-\alpha) \dot{\theta}_f^T n_f \right) T d\tau \end{aligned} \tag{13}$$

The state equations (6) for $0 \le t \le \alpha T$ and (8) for $\alpha T \le t \le T$ are transformed onto τ -axis as follows.

$$\frac{dw_s}{d\tau} = \alpha T \begin{bmatrix} \dot{x}_s \\ H_s^{-1}(u_s - C_s\dot{x}_s - g_s) \end{bmatrix} \tag{14}$$

$$\frac{dw_f}{d\tau} = (\alpha - 1)T \begin{bmatrix} \dot{x}_f \\ H_f^{-1}(u_f - C_f\dot{x}_f - g_f) \end{bmatrix} \tag{15}$$

State variables should include the support phase ratio α in order to find its optimal value as well. The support phase ratio is constant. Then, the following differential equation is introduced.

$$\frac{d\alpha}{d\tau} = 0 \tag{16}$$

Finally, the problem (9)(10) is transformed into a Bolza problem.
minimize

$$\widetilde{E} = g(z_1) + \int_0^1 \left(f_0(z(\tau), v(\tau)) + \lambda(\tau)^T \left(\frac{dz(\tau)}{d\tau} - f(z(\tau), v(\tau)) \right) \right) d\tau \tag{17}$$

where $z = (w_s, w_f, \alpha) = (x_s, \dot{x}_s, x_f, \dot{x}_f, \alpha) = (\theta_s, \varphi_s, \dot{\theta}_s, \dot{\varphi}_s, \theta_f, \varphi_f, p_f, \dot{\theta}_f, \dot{\varphi}_f, \dot{p}_f, \alpha) \in \Re^{4N+19}$ is a state vector, $v = (n_s, n_f) \in \Re^{2N}$ is a input vector, $\lambda \in \Re^{4N+19}$ is a Lagrange multiplier, $z_1 = z(1)$ is state at the terminal period, and

$$f_0(z, v) = \left(\alpha \dot{\theta}_s^T n_s + (1 - \alpha) \dot{\theta}_f^T n_f \right) T \tag{18}$$

$$f(z, v) = \begin{bmatrix} \alpha T \dot{x}_s \\ \alpha T H_s^{-1}(u_s - C_s\dot{x}_s - g_s) \\ (\alpha - 1)T\dot{x}_f \\ (\alpha - 1)T H_f^{-1}(u_f - C_f\dot{x}_f - g_f) \\ 0 \end{bmatrix} \tag{19}$$

The function $g(z_1)$ represents penalty for the terminal condition that is introduced to guarantee continuity of the state variable at the instant of the taking-off.

$$\begin{aligned} g(z_1) = W \Big(& \left\| \theta_s(1) - \theta_f(1) \right\|^2 + \left\| \dot{\theta}_s(1) - \dot{\theta}_f(1) \right\|^2 + \left\| \varphi_s(1) - \varphi_f(1) \right\|^2 \\ & + \left\| \dot{\varphi}_s(1) - \dot{\varphi}_f(1) \right\|^2 + \left\| p_s(1) - p_f(1) \right\|^2 + \left\| \dot{p}_s(1) - \dot{p}_f(1) \right\|^2 \Big) \end{aligned} \tag{20}$$

where W is an weight coefficient. The variables p_s and $\dot{p}_s$ are implicitly defined, which are represented by functions of w_s. Variation of the extended objective function $\widetilde{E}$ is given by

$$\begin{aligned} \delta\widetilde{E} = & -\lambda_0^T \frac{\partial z_0}{\partial z_0'^T} \delta z_0' + \left(\frac{\partial g}{\partial z_1} + \lambda_1 \right)^T \delta z_1 + \int_0^1 \Bigg(\left(\frac{\partial f_0}{\partial z} - \frac{\partial f^{\mathrm{T}}}{\partial z} \lambda - \frac{d\lambda}{d\tau} \right)^T \delta z \\ & + \left(\frac{\partial f_0}{\partial v} - \frac{\partial f^{\mathrm{T}}}{\partial v} \lambda \right)^{\mathrm{T}} \delta v + \left(\frac{dz}{d\tau} - f \right)^{\mathrm{T}} \delta\lambda \Bigg) d\tau \end{aligned} \tag{21}$$

where $\lambda_0 = \lambda(0)$ and $\lambda_1 = \lambda(1)$. In this equation, we assume that the initial state z_0 is a function of certain variables which consist of partial set of the state, namely, a part of the initial state is independent and the other depends on it. Let the independent initial state variables be $z_0' = (\theta_s(0), \varphi_s(0), \dot{\theta}_f(0), \dot{\varphi}_f(0), \dot{p}_f(0), \alpha(0))$. The rest of the initial state are decided by

$$\theta_f(0) = K\theta_s(0) \tag{22}$$

$$\varphi_f(0) = \varphi_s(0) \tag{23}$$

$$p_f(0) = -h(\theta_s(0), \varphi_s(0)) + S \tag{24}$$

$$\begin{bmatrix} \dot{\theta}_s(0) \\ \dot{\varphi}_s(0) \end{bmatrix} = \begin{bmatrix} K & 0 & 0 \\ 0 & I & 0 \end{bmatrix} \left(I - H_f^{-1} \tilde{J}_f^T \left(\tilde{J}_f H_f^{-1} \tilde{J}_f^T \right)^{-1} \tilde{J}_f \right) \begin{bmatrix} \dot{\theta}_f(0) \\ \dot{\varphi}_f(0) \\ \dot{p}_f(0) \end{bmatrix} \tag{25}$$

The first three equations are coordinate conversion at the instant of landing and the last is the condition of perfectly inelastic collision at the instant of landing. Let the impulsive external force at the foot of support leg be δf. The impact force δf is inflicted at the instant of the landing and the generalized velocity changes discontinuously. From (1), the generalized momentum after the collision is given by

$$H\dot{x}_+ = H\dot{x}_- + \tilde{J}^T \delta f \tag{26}$$

where $\dot{x}_+$ and $\dot{x}_-$ denote the generalized velocities after and before collision, respectively. $\tilde{J} = [J, R, I]$ is an extended Jacobian. Since it is support phase after the collision, the condition (3) holds, namely,

$$\tilde{J}\dot{x}_+ = 0 \tag{27}$$

Describing (26) and (27) for $\dot{x}_+$ and δf, the following equation is obtained.

$$\begin{bmatrix} H & -\tilde{J}^T \\ -\tilde{J} & 0 \end{bmatrix} \begin{bmatrix} \dot{x}_+ \\ \delta f \end{bmatrix} = \begin{bmatrix} H\dot{x}_- \\ 0 \end{bmatrix} \tag{28}$$

Eliminating δf from (28), we have

$$\dot{x}_+ = \left(I - H^{-1} \tilde{J}^T \left(\tilde{J} H^{-1} \tilde{J}^T \right)^{-1} \tilde{J} \right) \dot{x}_- \tag{29}$$

Here, $\dot{x}_+$ corresponds to $\dot{x}_s(0)$ which is the generalized velocity of the support phase at $\tau = 0$, and $\dot{x}_-$ corresponds to $\dot{x}_f(0)$ which is the generalized velocity of the flight phase at $\tau = 0$. Taking into account the coordinate conversion between left and right leg, (29) is transformed into the form of (25).

From (21), the following conditions are obtained.

$$\lambda_1 = -\frac{\partial g}{\partial z_1} \tag{30}$$

$$\frac{d\lambda}{d\tau} = \frac{\partial f_0}{\partial z} - \frac{\partial f^T}{\partial z}\lambda \tag{31}$$

$$\frac{dz}{d\tau} = f \tag{32}$$

Also the gradients are given by

$$\frac{\partial \tilde{E}}{\partial z_0'} = -\frac{\partial z_0^T}{\partial z_0'}\lambda_0 \tag{33}$$

$$\frac{\partial \tilde{E}}{\partial v} = \frac{\partial f_0}{\partial v} - \frac{\partial f^T}{\partial v}\lambda \tag{34}$$

To find the optimal solution, the conjugate gradient method in infinite dimensional space (Hilbert space) is applied to this problem. The procedures of the algorithm are as follows.

1) The initial solution $(z_0', v(\tau))$ is given.
2) The initial state z_0 is computed by (22)-(25).
3) The differential equation (32) is solved using z_0 as the initial condition.
4) λ_1 is computed by (30) using the final value z_1.
5) The differential equation (31) is backwardly solved using z_1.
6) The gradients for z_0' and $v(\tau)$ are computed by (33)(34) using $z(\tau)$, $\lambda(\tau)$, and $v(\tau)$.
7) The temporary solution $(z_0', v(\tau))$ is updated toward the direction of the conjugate gradient.
8) If the gradient is not small enough, return to 2.

Finally, the input joint torques $n(t)$, the joint angles $\theta(t)$, the posture and position (of the base link) $\varphi(t)$, $p(t)$, their derivatives $\dot{\theta}(t)$, $\dot{\varphi}(t)$, and the support phase ratio α are obtained. A general method to compute the partial derivatives in (30)-(34) is proposed in the next section.

4. Computational Scheme for Partial Derivative

It is difficult to calculate the partial derivatives in (30)-(34) symbolically, because basically it costs very much to obtain a symbolic expression of the equation of motion (1). In this section, a computational scheme for the partial derivatives based on numerical representation of motion equation is proposed. Finally we can compute them easily by using forward-backward recursive Newton-Eular formulation.
Each partial derivative appeared in (30)-(34) is represented as follows.

$$\frac{\partial f}{\partial z^T} = T \times \begin{bmatrix} 0 & \alpha I & 0 & 0 & \dot{x}_s \\ \alpha \dfrac{\partial f_s}{\partial x_s^T} & \alpha \dfrac{\partial f_s}{\partial \dot{x}_s^T} & 0 & 0 & f_s \\ 0 & 0 & 0 & (\alpha-1)I & \dot{x}_f \\ 0 & 0 & (\alpha-1)\dfrac{\partial f_f}{\partial x_f^T} & (\alpha-1)\dfrac{\partial f_f}{\partial \dot{x}_f^T} & f_f \\ 0 & 0 & 0 & 0 & 0 \end{bmatrix} \tag{35}$$

where

$$f_s = H_s^{-1}\left(u_s - C_s\dot{x}_s - g_s\right) \tag{36}$$

$$f_f = H_f^{-1}\left(u_f - C_f\dot{x}_f - g_f\right) \tag{37}$$

And then,

$$\frac{\partial f_s}{\partial x_{si}} = -H_s^{-1}\left(\frac{\partial C_s}{\partial x_{si}}\dot{x}_s + \frac{\partial g_s}{\partial x_{si}}\right) - H_s^{-1}\frac{\partial H_s}{\partial x_{si}}f_s \tag{38}$$

$$\frac{\partial f_f}{\partial x_{fi}} = -H_f^{-1}\left(\frac{\partial C_f}{\partial x_{fi}}\dot{x}_f + \frac{\partial g_f}{\partial x_{fi}}\right) - H_f^{-1}\frac{\partial H_f}{\partial x_{fi}}f_f \tag{39}$$

$$\frac{\partial f}{\partial v^T} = \begin{bmatrix} 0 & 0 \\ \alpha T H_s^{-1} P_s & 0 \\ 0 & 0 \\ 0 & (\alpha - 1) T H_f^{-1} P_f \\ 0 & 0 \end{bmatrix} \tag{40}$$

where $P_s = [I,0]^T \in \Re^{(N+3)\times N}$, $P_f = [I,0,0]^T \in \Re^{(N+6)\times N}$ are selection matrices. And also,

$$\frac{\partial f_0}{\partial z} = \begin{bmatrix} 0 \\ 0 \\ \alpha T n_s \\ 0 \\ 0 \\ 0 \\ 0 \\ (1-\alpha) T n_f \\ 0 \\ 0 \\ T\left(\dot{\theta}_s^T n_s - \dot{\theta}_f^T n_f\right) \end{bmatrix} \tag{41}$$

$$\frac{\partial f_0}{\partial v} = \begin{bmatrix} \alpha T \dot{\theta}_s \\ (1-\alpha) T \dot{\theta}_f \end{bmatrix} \tag{42}$$

$$\frac{\partial z_0}{\partial z_0'^T} = \begin{bmatrix} I & 0 & 0 \\ \Gamma & \Lambda & 0 \\ \widetilde{K} & 0 & 0 \\ 0 & I & 0 \\ 0 & 0 & 1 \end{bmatrix} \tag{43}$$

$$\frac{\partial g}{\partial z_1} = 2W \times \begin{bmatrix} \theta_{s1} - \theta_{f1} + J_s^T\left(h_s + p_{f1}\right) + \left[\dot{\theta}_{s1}^T \dfrac{\partial J_s^T}{\partial \theta_{s1i}}\left(J_s\dot{\theta}_{si} + \dot{p}_{f1}\right)\right] \\ \varphi_{s1} - \varphi_{f1} + R_s^T\left(h_s + p_{f1}\right) + \left[\dot{\varphi}_{s1} \dfrac{\partial R_s^T}{\partial \varphi_{s1i}}\left(R_s\dot{\varphi}_{s1} + \dot{p}_{f1}\right)\right] \\ \dot{\theta}_{s1} - \dot{\theta}_{f1} + J_s^T\left(J_s\dot{\theta}_{s1} + \dot{p}_{f1}\right) \\ \dot{\varphi}_{s1}^T - \dot{\varphi}_{f1} + R_s^T\left(R_s\dot{\varphi}_{s1} + \dot{p}_{f1}\right) \\ -\theta_{s1} + \theta_{f1} \\ -\varphi_{s1} + \varphi_{f1} \\ h_s + p_{f1} \\ -\dot{\theta}_{s1} + \dot{\theta}_{f1} \\ -\dot{\varphi}_{s1} + \dot{\varphi}_{f1} \\ J_s\dot{\theta}_{s1} + \dot{p}_{f1} \\ 0 \end{bmatrix} \tag{44}$$

where the subscript 1 corresponds to the value at $\tau = 1$, and

$$\widetilde{K} = \begin{bmatrix} K & 0 \\ 0 & I \\ -J_s & -R_s \end{bmatrix} \tag{45}$$

$$\Lambda = \widetilde{K}_l\left(I - H_f^{-1}\widetilde{J}_f^T\left(\widetilde{J}_f H_f^{-1}\widetilde{J}_f^T\right)^{-1}\widetilde{J}_f\right) \tag{46}$$

$$\widetilde{K}_l = \begin{bmatrix} K & 0 & 0 \\ 0 & I & 0 \end{bmatrix} \tag{47}$$

$$\Gamma = \left[\frac{\partial \Lambda}{\partial x_{si}}\dot{x}_f\right] \tag{48}$$

$$\frac{\partial \Lambda}{\partial x_{si}} = \widetilde{K}_l H_f^{-1}\frac{\partial H_f}{\partial x_{fi}}H_f^{-1}\widetilde{J}_f^T\Omega\widetilde{J}_f - H_f^{-1}\frac{\partial \widetilde{J}_f^T}{\partial x_{fi}}\Omega\widetilde{J}_f - H_f^{-1}\widetilde{J}_f^T\Omega\frac{\partial \widetilde{J}_f^T}{\partial x_{fi}}$$
$$+ H_f^{-1}\widetilde{J}_f^T\Omega\left(\frac{\partial \widetilde{J}_f}{\partial x_{fi}}H_f^{-1}\widetilde{J}_f^T - \widetilde{J}_f H_f^{-1}\frac{\partial H_f}{\partial x_{fi}}H_f^{-1}\widetilde{J}_f^T + \widetilde{J}_f H_f^{-1}\frac{\partial \widetilde{J}_f^T}{\partial x_{fi}}\right)\Omega\widetilde{J}_f\widetilde{K}_r \tag{49}$$

$$\Omega = \left(\widetilde{J}_f H_f^{-1}\widetilde{J}^T\right)^{-1} \tag{50}$$

$$\widetilde{K}_r = \begin{bmatrix} K & 0 \\ 0 & I \\ 0 & 0 \end{bmatrix} \tag{51}$$

The partial derivatives appeared in (38), (39), (44), (48), and (49) are computed by using modified Newton-Euler formulations.

5. Numerical Study of Five-link Planar Biped

The proposed method is applied to a five-link planar biped robot. The specification of the robot and the control parameters are shown in Table 1. The robot is 1.2 [m] height and 60 [kg] weight. The coordinates are taken as shown in Fig. 1.
The optimal trajectories are computed as shown in Fig. 3-Fig. 6. Snapshots of the running motion are also shown in Fig. 7. The solid lines and the dashed lines show the trajectories for the right leg and the left leg, respectively. In Fig. 4, there are some discontinuous velocities due to the impact force at the instant of the landing. In Fig. 5, the peak torque for the hip joints appears at the beginnings of the swinging. For the knee joints, the torque becomes maximal at the instant of the landing and keeps over 100N.m. In Fig. 6, the positive peak power for the hip and knee joints appears during kicking motion. For the hip joints, the power becomes negative peak value at the beginning of the flight phase. This means that the hip joints absorb the energy of the kicking motion. The negative peak power for the knee joints appears at the instant of the landing. Namely, knee joints absorb the impact power between the foot and the ground.

body length and weight	0.6m, 20kg
thigh length and weight	0.3m, 10kg
shin length and weight	0.3m, 10kg
total height & weight	1.2m, 60kg
stride S	0.5m
period of one step T	0.5s
running speed T/S	1m/s

Table 1. Specifications of robot and control parameters.

	hip	knee
peak angular velocity [rad/s]	14.5	11.6
peak torque [N.m]	48.2	117.6
peak power (positive) [W]	355	1265
peak power (negative) [W]	-699	-849
consumption power [W]	27.9	-5.37
total consumption power [W]	45.1	

Table 2. Actuator requirement.

Table 2 shows requirements for the actuators based on this result. It is found that very big power is required for knee joints. However, its total consumption power has small negative value. Therefore, the main work is done by the hip joints. Since the negative power is also

big, for real robots, the introduction of the energy regeneration mechanism such as elastic actuators or combination of high back-drivable actuators and bidirectional power converters is effective to reduce the total consumption power.

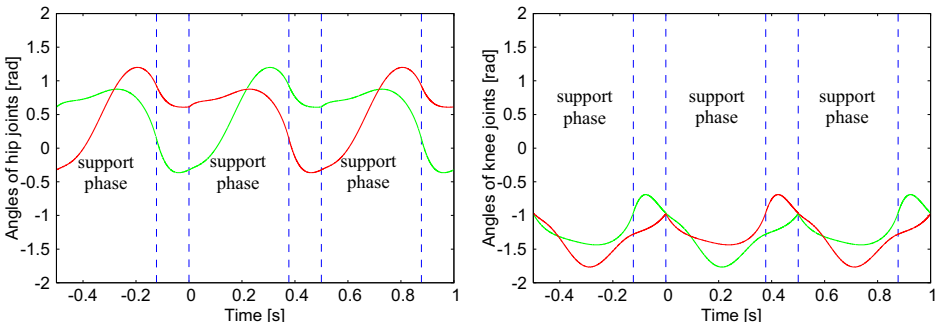

(a) hip joint (b) knee joint.

Fig. 3. Joint angles (solid line: right leg, dashed line: left leg).

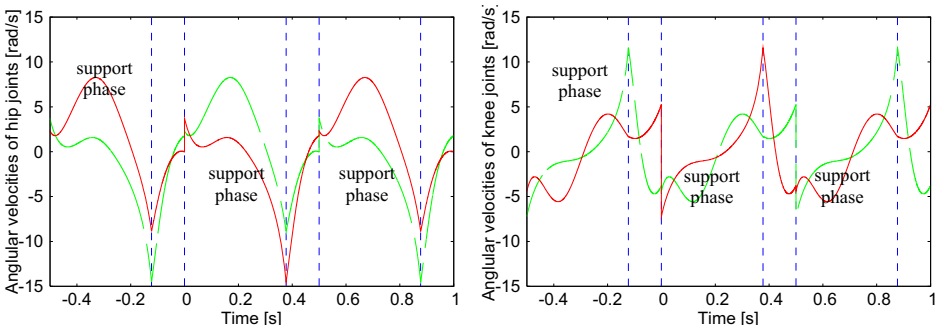

(a) hip joint (b) knee joint.

Fig. 4. Angular velocities of joints (solid line: right leg, dashed line: left leg).

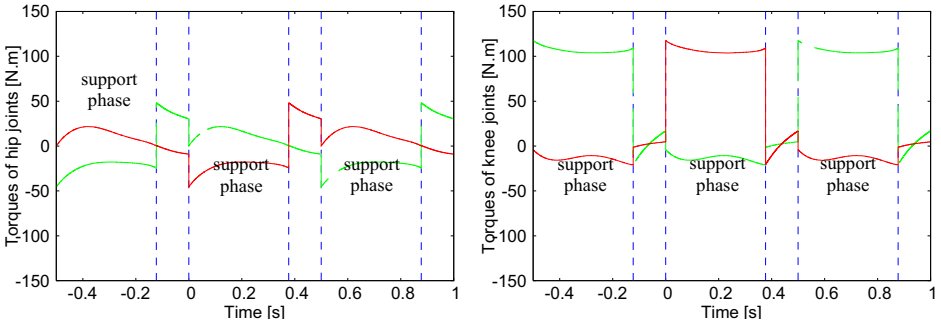

(a) hip joint (b) knee joint.

Fig. 5. Joint torques (solid line: right leg, dashed line: left leg).

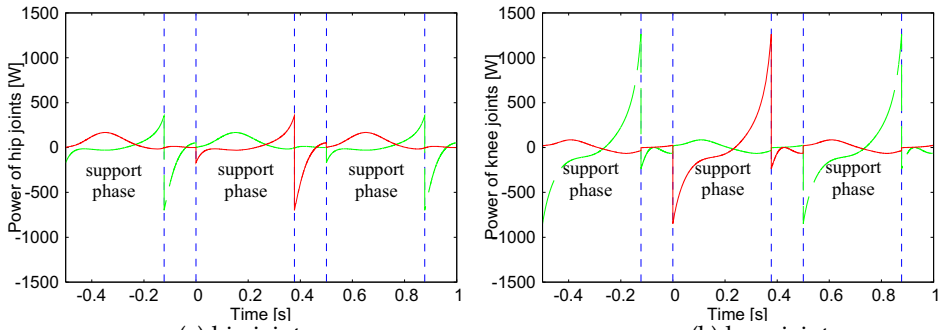

(a) hip joint (b) knee joint.

Fig. 6. Joint powers (solid line: right leg, dashed line: left leg).

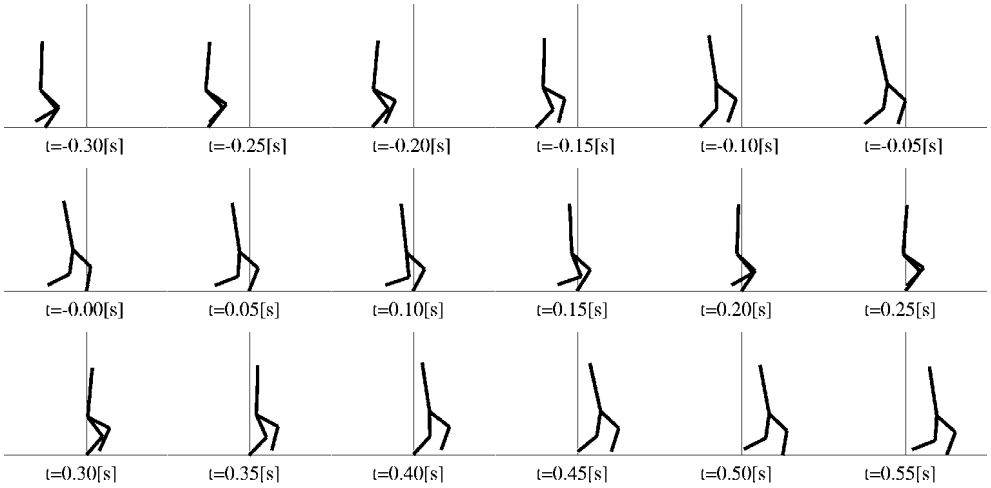

Fig. 7. Snapshots of running trajectory.

6. Conclusion

In this chapter, the method to generate a trajectory of a running motion with minimum energy consumption is proposed. It is useful to know the lower bound of the consumption energy when we design the bipedal robot and select actuators. The exact and general formulation of optimal control for biped robots based on numerical representation of motion equation is proposed to solve exactly the minimum energy consumption trajectories. Through the numerical study of a five link planar biped robot, it is found that big peak power and torque is required for the knee joints but its consumption power is small and the main work is done by the hip joints.

8. References

Fujimoto, Y. & Kawamura, A. (1995). Three Dimensional Digital Simulation and Autonomous Walking Control for Eight-axis Biped Robot, *Proceedings of IEEE*

International Conference on Robotics and Automation, pp. 2877-2884, 0-7803-1965-6, Nagoya, May 1995, IEEE, New York

Fujimoto, Y. & Kawamura, A. (1998). Simulation of an Autonomous Biped Walking Robot Including Environmental Force Interaction, *IEEE Robotics and Automation Magazine*, Vol. 5, No. 2, June 1998, pp. 33–42, 1070-9932

Goswami, A. (1999). Foot-Rotation Indicator (FRI) Point: A New Gait Planning Tool to Evaluate Postural Stability of Biped Robot, *Proceedings of IEEE International Conference on Robotics and Automation*, pp. 47-52, 0-7803-5180-0, Detroit, May 1999, IEEE, New York

Hirai, K.; Hirose, M.; Haikawa, Y. & Takenaka, T. (1998). TheDevelopment of Honda Humanoid Robot, *Proceedings of IEEE International Conference on Robotics and Automation*, pp. 1321-1326, 0-7803-4300-X, Leuven, May 1998, IEEE, New York

Hodgins, J. K. (1996). Three-Dimensional Human Running, *Proceedings of IEEE International Conference on Robotics and Automation*, pp. 3271-3277, 0-7803-2988-0, Minneapolis, April 1996, IEEE, New York

Kajita, S.; Nagasaki, T.; Yokoi, K.; Kaneko, K. & Tanie, K. (2002). Running Pattern Generation for a Humanoid Robot, *Proceedings of IEEE International Conference on Robotics and Automation*, pp. 2755-2761, 0-7803-7272-7, Washington DC, May 2002, IEEE, New York

Kajita, S.; Kanehiro, F.; Kaneko, K.; Fujiwara, K.; Harada, K.; Yokoi, K. & Hirukawa, H. (2003). Biped Walking Pattern Generation by using Preview Control of Zero-Moment Point, *Proceedings of IEEE International Conference on Robotics and Automation*, pp. 1620–1626, 0-7803-7736-2, Taipei, May 2003, IEEE, New York

Kaneko, K.; Kanehiro, F.; Kajita, S.; Hirukaka, H.; Kawasaki, T.; Hirata, M.; Akachi, K. & Isozumi, T. (2004). Humanoid Robot HRP-2, *Proceedings of IEEE International Conference on Robotics and Automation*, pp. 1083-1090, 0-7803-8232-3, New Orleans, April 2004, IEEE, New York

Loffler, K.; Gienger, M. & Pfeiffer, F. (2003). Sensor and Control Design of a Dynamically Stable Biped Robot, *Proceedings of IEEE International Conference on Robotics and Automation*, pp. 484-490, 0-7803-7736-2, Taipei, May 2003, IEEE, New York

Nagasaki, T.; Kajita, S.; Kaneko, K.; Yokoi, K. & Tanie, K. (2004). A Running Experiment of Humanoid Biped, *Proceedings of IEEE/RSJ International Conference on Intelligent Robots and Systems*, pp. 136-141, 0-7803-8463-6, Sendai, September 2004, IEEE, New York

Nishiwaki, K.; Kagami, S.; Kuffner J. J.; Inaba, M. & Inoue, H. (2003). Online Humanoid Walking Control System and a Moving Goal Tracking Experiment, *Proceedings of IEEE International Conference on Robotics and Automation*, pp. 911-916, 0-7803-7736-2, Taipei, May 2003, IEEE, New York

Raibert, M., H. (1986). *Legged Robots That Balance*, MIT Press, 0-262-18117-7, Cambridge

Roussel, L.; Canudas-de-Wit, C. & Goswami, A. (1998). Generation of Energy Optimal Complete Gait Cycles for Biped Robots, *Proceedings of IEEE International Conference on Robotics and Automation*, pp. 2036–2041, 0-7803-4300-X, Leuven, May 1998, IEEE, New York

Sugahara, Y.; Endo, T.; Lim, H. & Takanishi, A. (2003). Control and Experiments of a Multi-purpose Bipedal Locomotor with Parallel Mechanism, *Proceedings of IEEE*

International Conference on Robotics and Automation, pp. 4342-4347, 0-7803-7736-2, Taipei, May 2003, IEEE, New York

Vukobratovic, M.; Borovac, B. & Surdilovic, D. (2001). Zero-Moment Point - Proper Interpretation and New Applications, *Proceedings of International Conference on Humanoids Robots*, pp. 237-244, 4-9901025-0-9, Tokyo, November 2001, IEEE, New York

Yamaguchi, J.; Soga, E.; Inoue, S. & Takanishi, A. (1999). Development of a Bipedal Humanoid Robot—Control Method of Whole Body Cooperative Dynamic Biped Walking, *Proceedings of IEEE International Conference on Robotics and Automation*, pp. 368-374, 0-7803-5180-0, Detroit, May 1999, IEEE, New York

Humanoid Robots: New Developments

Edited by Armando Carlos de Pina Filho

ISBN 978-3-902613-00-4
Hard cover, 582 pages
Publisher I-Tech Education and Publishing
Published online 01, June, 2007
Published in print edition June, 2007

For many years, the human being has been trying, in all ways, to recreate the complex mechanisms that form the human body. Such task is extremely complicated and the results are not totally satisfactory. However, with increasing technological advances based on theoretical and experimental researches, man gets, in a way, to copy or to imitate some systems of the human body. These researches not only intended to create humanoid robots, great part of them constituting autonomous systems, but also, in some way, to offer a higher knowledge of the systems that form the human body, objectifying possible applications in the technology of rehabilitation of human beings, gathering in a whole studies related not only to Robotics, but also to Biomechanics, Biomimmetics, Cybernetics, among other areas. This book presents a series of researches inspired by this ideal, carried through by various researchers worldwide, looking for to analyze and to discuss diverse subjects related to humanoid robots. The presented contributions explore aspects about robotic hands, learning, language, vision and locomotion.

How to reference

In order to correctly reference this scholarly work, feel free to copy and paste the following:

Yasutaka Fujimoto (2007). Minimum Energy Trajectory Planning for Biped Robots, Humanoid Robots: New Developments, Armando Carlos de Pina Filho (Ed.), ISBN: 978-3-902613-00-4, InTech, Available from: http://www.intechopen.com/books/humanoid_robots_new_developments/minimum_energy_trajectory_planning_for_biped_robots

INTECH
open science | open minds

InTech Europe
University Campus STeP Ri
Slavka Krautzeka 83/A
51000 Rijeka, Croatia
Phone: +385 (51) 770 447
Fax: +385 (51) 686 166
www.intechopen.com

InTech China
Unit 405, Office Block, Hotel Equatorial Shanghai
No.65, Yan An Road (West), Shanghai, 200040, China
中国上海市延安西路65号上海国际贵都大饭店办公楼405单元
Phone: +86-21-62489820
Fax: +86-21-62489821